Light Attenuation and Color Fluctuation for Underwater Image Restoration *

Jingchun Zhou[1 [0000−0002−4111−6240]], Dingshuo Liu[1 [0000−0001−9821−2455]], Dehuan Zhang[1 [0000−0002−2987−9528]], and Weishi Zhang[1 [0000−0003−0519−8397]]

Dalian Maritime University, 1 Linghai Road, Dalian 116026, China
teesiv@dlmu.edu.cn

Abstract. Underwater images with low contrast and color distortion of different scenarios often pose a significant challenge in improving underwater image quality. Therefore, it is beneficial to restore the real restoration effect of the scene by estimating the degradation parameters related to their changes, and these parameters should be updated with the degradation scene to obtain the best visual effect. We propose a robust underwater image restoration method. Specifically, we adjust the color of the input image according to a background light (BL) estimation strategy guided by depth, chromatic aberration considering hue, and information entropy. At the same time, we adjust the depth map of the input image by computing color fluctuation and attenuation. According to qualitative and quantitative evaluation, the proposed method generates vivid results with a more natural appearance and more valuable information.

Keywords: Underwater image restoration · Background light · Depth map · Color fluctuation.

1 Introduction

Underwater vision is critical for mining marine resources and conducting marine surveys. Due to light absorption and dispersion, underwater images acquired by optical cameras may suffer from color distortion and diminished contrast [1–6]. The degraded image and histogram are shown in Fig. 1. However, light is deflected before reaching the camera due to the excitation of particles present in the water, resulting in visual issues such as haze, and low contrast in the acquired images. The accuracy of vision tasks such as underwater object detection and segmentation suffers as a result of these image quality degradations. Hence, underwater image restoration is important for a variety of vision-based applications in underwater situations [7–11].

* This work was supported in part by the National Natural Science Foundation of China (No. 61702074), the Liaoning Provincial Natural Science Foundation of China (No. 20170520196), and the Fundamental Research Funds for the Central Universities (Nos.3132019205 and 3132019354).

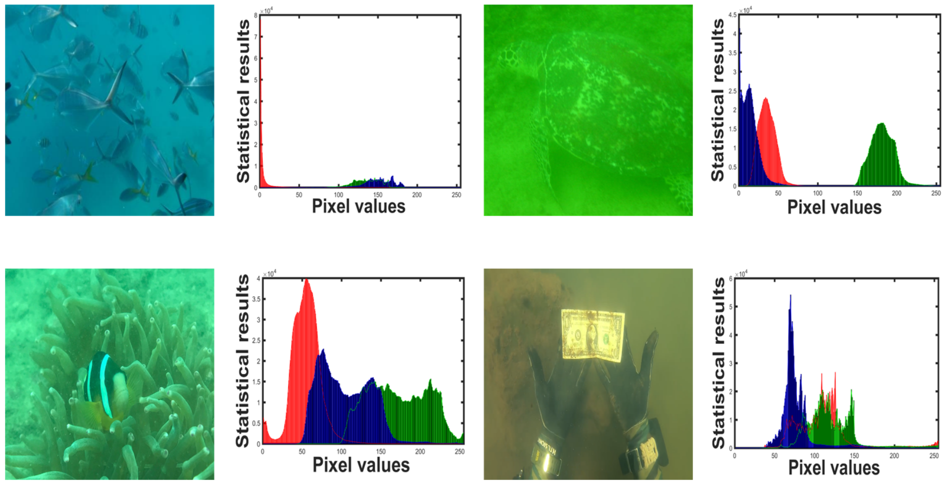

Fig. 1. The degraded images and histograms.

Other underwater applications, such as underwater item detection, object segmentation, and biological tracking, frequently use underwater image enhancement techniques as a pre-processing step. As a result, many approaches for restoring underwater pictures of diverse situations and degrees of degradation have been developed. The generality of previous approaches is frequently insufficient due to erroneous background light and transmission estimation. There is still a lot of work to be done on the details to solve the problem of color shift, decreased contrast, and details disappearance. As a result, based on background light estimation and transmission estimation, this research provides an underwater image restoration approach. Based on the degree of entropy, depth, and color difference, including hue, we develop a background light estimation model. We establish the depth map of the input image by computing color fluctuation and attenuation. Transmission maps (TM) obtained by accurate depth map calculations tend to retain more details, have higher contrast, and have better visual effects.

The technical contributions of this paper are summarized as follows:

1) In this work, we propose a novel estimate method for BL that consider bright and dark channel differences, color differences, and information entropy. Although the difference between bright and dark channels is an essential metric for depth, it is not the only clue for underwater. The blurred region [12] at infinity contains less information, and entropy is the key evaluation metric. When the difference between different color channels is large, the differential absorption of red light can be used. The BL of our method is more accurate, which effectively solves the wrong estimate of BL when there are white objects in the foreground by the DCP-based [13, 14] method.

2) We calculate the color fluctuation and attenuation to estimate the scene depth. The deeper the scene depth, the larger the color attenuation. Previous

work [12, 15, 16] suggested that the red channel attenuates strongly with increasing depth, but this leads to failure in some specific scenes. Our method not only estimates depth by color channels but also considers light scattering. Using an accurate depth map to yield a computed transmission map improves the contrast and preserves more edge detail.

3) We report the qualitative and quantitative evaluation of our method and existing methods in natural underwater scenes. The performance of contrast enhancement and removal of color distortion is demonstrated by our method outperforms existing state-of-the-art methods.

The remainder of the paper is structured as follows. The methods for current image processing are discussed in Section 2. The proposed approach is described in Section 3. Section 4 presents experimental findings, while Section 5 presents conclusions.

2 Related Work

underwater image enhancement methods include the Model-free method, the Model-based method, and the Deep learning-based method.

2.1 Model-free method

Color correction and contrast improvement are typically possible using underwater image enhancement technologies based on the non-physical model by changing pixel values. The novel method to improve underwater image quality was proposed by Zhuang et al. [17]. Bayesian retinex underwater image enhancement is proposed to improve visual effect (BRUIE). To reduce the influence of noise, Huang et al. [18] created relative global histogram stretching. However, the color correction approach is frequently insufficient to repair it (RGHS). Fu et al. [19] developed a mean and mean square error-based enhancement (RBE) approach for histogram equalization. However, when restoring underwater images, techniques based on statistical methods often lead to over-enhancement or artifacts and noise. Underwater image enhancement methods based on nonphysical models do not consider the scattering and attenuation of light, but directly adjust the pixels, usually resulting in excessive enhancement.

2.2 Model-based method

To remove fog in a single degraded image, Peng et al. [14] proposed the generalization of the dark channel prior (GDCP). In [16], the underwater light attenuation prior (ULAP) is used to estimate the scene's depth map and background light. Lee et al. [20] introduced an image-adaptive weighting factor to estimate the transmission map. Recently, a robust model for background light estimation and a new underwater dark channel prior was used to address the severe quality degradation and color distortion of underwater images [16]. Zhou et al. [21] suggested quadratic guided filtering into image restoration to obtain underwater images with the most realistic and natural appearance. Li et al. [3] proposed an underwater image restoration method based on blue-green channel dehazing and red channel correction (GBDRC). Due to the separate enhancement effect of the red channel, it usually leads to the over-saturation of red in the restoration results. This work presents an efficient program for underwater restoration. Our method effectively solves the underexposure of the restoration result caused by the large estimated value of the BL when the bright pixels are in the foreground [13, 22, 23]. Most restoration methods obtain transmission maps by using twice the minimum filter [13, 22, 23], which will cause the restoration result details to disappear. We establish the depth map of the input image by computing color fluctuation and attenuation. The previous methods [12, 15, 16] considered that the red value decreases with increasing depth. However, this prior approach fails in the special case. The proposed method considers the influence of light scattering. Transmission maps obtained by accurate depth maps tend to retain more details, have higher contrast, and have better visual effects.

2.3 Deep learning-based method

With the development of science and technology, the application of deep learning in underwater image enhancement tasks is more and more common. The restored scene using the depth learning method of Water-net [24] is dark, and the contrast has not been significantly improved. Li et al. [25] designed a network structure supported by underwater scene priors that offer good adaptability for various underwater scenarios (UWCNN). Li et al. [26] trained a multi-color spatial embedding network driven by media transmission. The current depth learning method network model generalization ability is limited, and can not be applied to a variety of underwater scenes, so there are still shortcomings in enhancing the ability.

3 Proposed method

This paper proposed a robust underwater image restoration method, the overall flow chart is displayed in Fig. 2. First, we design a background light estimation model that relies on prior features for depth, chromatic aberration, hue, and information entropy. Next, the depth map of the input image is roughly computed based on color fluctuation and attenuation. The transmission map obtained from the accurate depth map can retain more details of the image. The restored results improve the contrast while preserving the more valuable details. Ours qualitatively and quantitatively performs better than the existing methods, and the performance of contrast enhancement and color distortion removal is demonstrated by our method outperforming existing state-of-the-art methods.

3.1 Background Light Estimation

We usually use flat pixels away from the camera as background light estimates, hence estimating the background light (BL) involves considering depth informa-

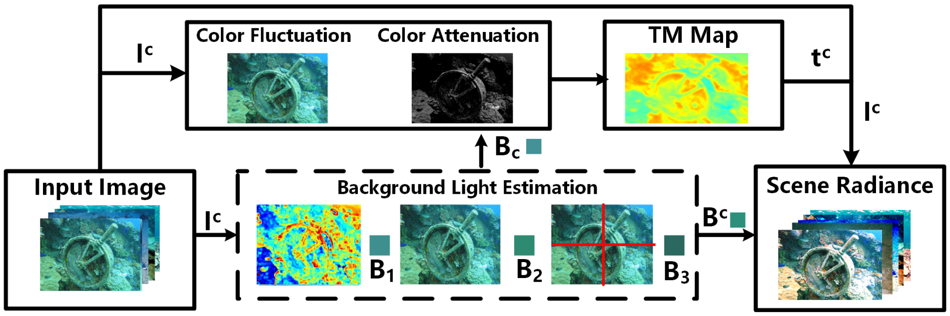

Fig. 2. Overview of the proposed method. We adjust the input color according to the background light through three background light candidates. At the same time, we estimate the depth map of the input image by calculating color fluctuations and attenuation.

tion. In addition, the background light region is blurred [12] and usually has less texture detail. The information entropy value is adopted to solve this problem, and the smaller value suggests that there is less information. In underwater conditions, red light has a longer wavelength, the blue and green light have shorter wavelengths. The red light is more attenuated than the blue and green light. The greater the chroma, the more depth in the field. In addition, we judge the dominant color of the degraded image and utilize the background light estimation to remove the influence of white objects or bright pixel areas in the foreground with higher robustness. First, the difference between light and dark channels can be used to estimate the depth. The greater the depth of the scene, the greater the difference in the intensity of light of different colors. If you make a difference between the light and dark channels, you can get the intensity difference of light of different colors. The farther the scene is from the camera, the greater the difference between light and dark channels. The bright channel I_{bright} and the dark channel I_{dark} are written as:

$$I_{bright}\left(x\right) = \max_{y\in\Omega(x)}\left(\max_{c\in\{r,g,b\}} I_c\left(y\right)\right) \tag{1}$$

$$I_{bright}\left(x\right) = \min_{y\in\Omega(x)}\left(\min_{c\in\{r,g,b\}} I_c\left(y\right)\right) \tag{2}$$

where $I_c\left(y\right)$ means the raw image and $\Omega\left(x\right)$ represent the local area of the input image where the pixel x is located. I_{bright} and I_{dark} are used in the estimation of the depth I_{depth}:

$$I_{depth}\left(x\right) = \ I_{bright}\left(x\right) - I_{dark}\left(x\right) \tag{3}$$

In addition, using the histogram stretching method to increase the contrast of the image:

$$I_{depth_{hs}}\left(x\right) = \frac{I_{depth}\left(x\right) - \min\left(I_{depth}\left(x\right)\right)}{\max\left(I_{depth}\left(x\right)\right) - \min\left(I_{depth}\left(x\right)\right)} \tag{4}$$

Calculated from the top 0.1 % of the brightest pixels, the background light candidate value B_1 can be expressed as:

$$B_1 = \frac{1}{\left|P^{0.1\%}_{I_{depth_{hs}}}\right|} I^c \left(\arg \max_{x \in P^{0.1\%}} \sum_{c \in \{r,g,b\}} I_{depth_{hs}}(x) \right) \tag{5}$$

where $P^{0.1\%}_{I_{depth_{hs}}}$ represents the top 0.1% of the brightest pixels. The second candidate for the background light is based on the hue considered the chromatic aberration, we define the dominant hue of the raw image:

$$I^B_{mean} > I^G_{mean}\; Bluish\, tone \tag{6}$$

$$I^B_{mean} \leq I^G_{mean}\; Greenish\, tone \tag{7}$$

where I^B_{mean} and I^G_{mean} are the average of the blue and green channel's intensity of the degraded images. The largest difference between blue/green and red channels is used as the second candidate value of the background light. I represents the original image.

$$B_2 = I\left[\max\left(I^B(x) - I^R(x)\right)\right]\; Bluish\, tone \tag{8}$$

$$B_2 = I\left[\max\left(I^G(x) - I^R(x)\right)\right]\; Greenish\, tone \tag{9}$$

The third candidate value of the background light has relied on information entropy. After the image has been divided into quadrants, it is estimated by calculating the local entropy in each image patch. Information entropy is described as follows:

$$E(i) = \sum_{i=0}^{N} P_y(i) \log_2 \left(P_y(i)\right) \tag{10}$$

where $P_y(i)$ represent the the i^{th} pixel of the local patch. N is the maximum of the pixel values. The background light is selected from a smooth area at infinity, and the smooth area corresponds to lower information entropy. The lower information entropy area was obtained after looping once using the quadtree algorithm:

$$B_3 = \frac{1}{m \times n} \sum\nolimits_{x \in \Omega(u)} C(x) \tag{11}$$

where $\Omega(u)$ represents the area with the minimum information entropy and $m \times n$ represents the total number of pixels in the area with the largest degree of smoothness.

$$B_{max} = \max\left(B_1, B_2, B_3\right) \tag{12}$$

$$B_{min} = \min\left(B_1, B_2, B_3\right) \tag{13}$$

Where B_{max}, B_{min} represent maximum and minimum value of B_1,B_2,B_3, respectively. We propose a background light estimation model:

$$a = \frac{|I > 0.5|}{I_{height} * I_{width}} \tag{14}$$

$$T(a, \xi) = \frac{1}{1 + e^{u(a-\xi)}} \tag{15}$$

$$\eta = T(a, \xi) \tag{16}$$

$$B = \eta * B_{\max} + (1 - \eta) * B_{\min} \tag{17}$$

where $I_{height} * I_{width}$ represents the total number of pixels in the input image, $|I > 0.5|$ means the number of bright pixels, a means the percentage of bright pixels in the input image. The value of ξ is 0.2, which is used to determine the brightness of the image. The empirical values of u are set to -32. Take the example of an image captured in a well-lit scene. When a $>\xi$, the degraded image was captured in a well-lit environment, and the obtained value of the background light is brighter, so a larger weight η is applied to $B_{\max}$. Fig.3 and Fig.4 display the background light estimation, the restoration results, RGB color map of the proposed method based on B and each background light candidate B_1, B_2, B_3, we can observe that by adopting our method as the background light, the results obtained have the best visual effect and color distribution.

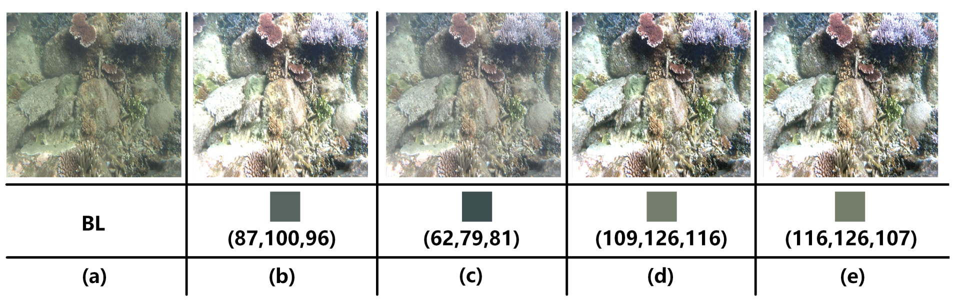

Fig. 3. Recovery results of different BL estimations. (a) The input image, (b)-(d) are the recovered images acquired by separately B_1, B_2, B_3, (e) our result.

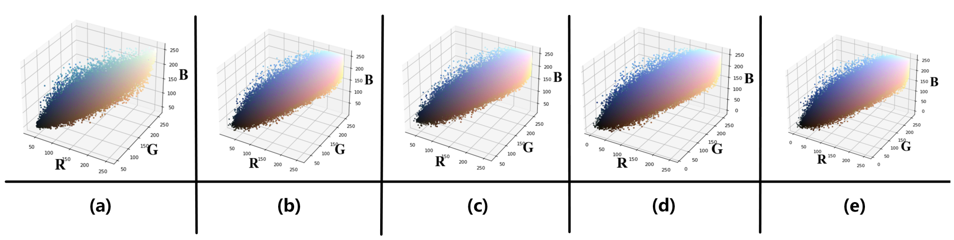

Fig. 4. The RGB space map of different BL estimations. (a) The input image, (b)-(d) are the RGB space maps acquired by separately B_1, B_2, B_3, (e) our result.

3.2 Depth Estimation

For depth map estimation, it is also characterized by smoothness and stability in large depth-of-field regions. The larger the depth of field, the more stable pixel in the sub-region. Brightness is brighter and saturation is susceptible to rapid decrease when there are many suspended particles. The difference between brightness and saturation (color degradation) is positively correlated with depth. First, we use color fluctuation to estimate the depth. The color fluctuation is written as follows:

$$S = k\sqrt{\frac{(r-m)^2 + (g-m)^2 + (b-m)^2}{3}}, m = \frac{r+g+b}{3} \tag{18}$$

where m represents the average value of the three channels of a single pixel, and k is the scale coefficient, which is taken as 30 here. In areas with higher depth of field, more stable pixels and fewer color fluctuations. Our first depth map is estimated to be as follows:

$$H_s(T) = \frac{T - \min(T)}{\max(T) - \min(T)} \tag{19}$$

$$d_{D_1} = 1 - H_s(S) \tag{20}$$

where T is a vector. Our second depth map relies on the degree of color attenuation [27], the saturation of the image is gradually reduced by the haze, while the brightness will increase. The difference between saturation and brightness is positively related to the depth of the scene.

$$C(x) = I^v(x) - I^s(x) \tag{21}$$

$$I^v(x) = \max_{c\in\{r,g,b\}} I^c(x) \tag{22}$$

$$I^s(x) = \left(\max_{c\in\{r,g,b\}} I^c(x) - \min_{c\in\{r,g,b\}} I^c(x)\right) / \max_{c\in\{r,g,b\}} I^c(x) \tag{23}$$

where $I^v(x)$ and $I^s(x)$ represent the brightness and saturation of the HSV space. where $C(x)$ used for the estimation of the depth map:

$$d_{D_2} = H_s(C) \tag{24}$$

An estimation method for depth is proposed:

$$d(x) = \mu_2 * d_{D_2} + \mu_1 * d_{D_1} \tag{25}$$

$$T(a, \xi) = \frac{1}{1 + e^{u(a-\xi)}} \tag{26}$$

$$\mu_1 = T(avg(B^c), 0.5) \tag{27}$$

$$\mu_2 = T(avg(I^r), 0.1) \tag{28}$$

In Eq. 27 and 28, the two parameters μ_1, μ_2 measure the brightness of the image and the intensity of the red channel respectively. When the underwater image scene is dark, the color fluctuation is not obvious, so d_1 cannot represent the change of depth, and a small weight μ_1 is applied to d_1 at this time. When there is a certain red component in the underwater image since the background light occupies more of the observed intensity of the scene points farther from the camera, the far scene points may still have larger values in the red channel, so the depth map d_2 applies a larger weight μ_2. As can be seen from Figure 5, the depth map obtained by our method most accurately expresses the depth information of underwater images and successfully separates the foreground and background.

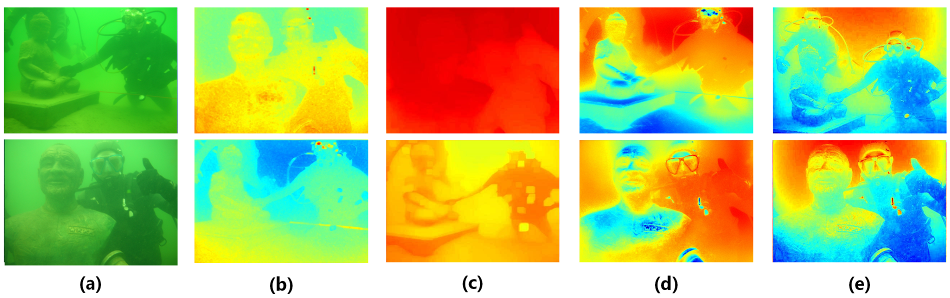

Fig. 5. Depth map comparison test. (a) Input image, (b)-(d) are the depth maps acquired by separately [15, 14, 16], (e) our result.

The distance between the camera and the nearest scene point can be expressed as:

$$d_0 = 1 - \max_{x,c\in\{r,g,b\}} \frac{\max |\ B_c\ - I^c\,(x)|}{\max\,(B^k, 1 - B^k)} \tag{29}$$

The final depth map of the underwater image is as follows:

$$d_{f(x)} = D \times (d_0 + d\,(x)) \tag{30}$$

where the constant D is utilized to translate relative distances into real distances. The following is an estimated transmission map for the red channel:

$$t^r\,(x) = e^{-\beta^r d_{f(x)}} \tag{31}$$

where β^r is the red channel attenuation coefficient, $\beta^r \in \left[\frac{1}{8}, \frac{1}{5}\right]$ [28]. In [29], the connection between both the attenuation coefficients of various color channels is demonstrated using the special optical characteristics of water as follows:

$$\frac{\beta^k}{\beta^r} = \frac{B^r\left(m\lambda^k{+}i\right)}{B^k\left(m\lambda^r{+}i\right)}, k \in \{g, b\} \tag{32}$$

where m=-0.00113, i=1.62517, and λ is the wavelength of the three color channels. The transmission map of the additional blue and green channels can be written as follows:

$$t^g(x) = t_f^r(x)^{\frac{\beta^g}{\beta^r}} \tag{33}$$

$$t^b(x) = t_f^r(x)^{\frac{\beta^b}{\beta^r}} \tag{34}$$

Fig. 6 shows a comparative experiment of the transmission maps estimated by the four restoration models. The transmission map obtained by dark channel prior (DCP) [13] is difficult to distinguish foreground from background. The overall transmission of the restoration method is based on image blurriness and light absorption (IBLA) [12], and the proposed method is more accurate. The transmission map obtained by GDCP [14] is smaller due to the larger distance between the camera and objects in the foreground estimated by GDCP. Our method estimates the transmission map to correctly express scene depth while retaining more valuable details.

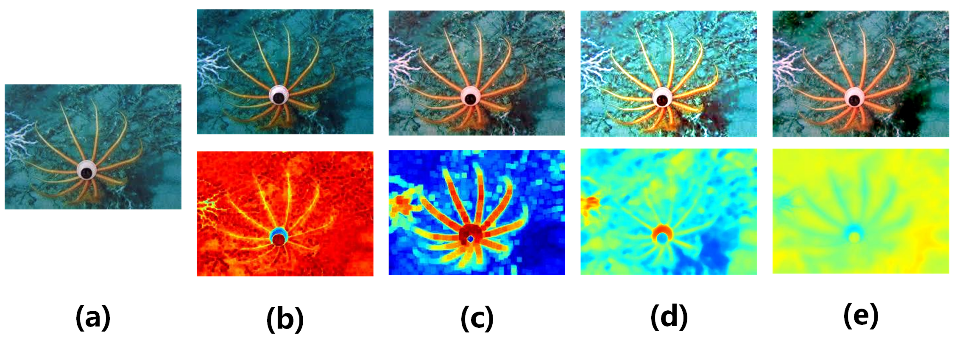

Fig. 6. Transformation maps comparison tests. (a) Input image, (b) DCP[13], (c) IBLA[12], (d) GDCP[14], (e) Our method.

The following is the final restoration equation:

$$J^c(x) = \frac{I^c(x) - B^c(x)}{\min\left(\max\left(t^c(x), 0.05\right), 0.95\right)} + B^c, c \in \{r, g, b\} \tag{35}$$

where the adjusted image is shown by $J^c(x)$. The white balance method is used in the suggested color correction and is based on the ideal gain factor [30].

4 Experiments and results

The suggested method enhances the regional features of the image, for instance, the texture features of the sculptures and plates, in the red-marked area of Fig. 7. Fig. 8 (a) displays the before-and-after comparison diagram. High-intensity pixels are corrected for the red and green channels (as shown in Fig. 8), while the green channel's pixel intensity values are decreased. As a result, the color sense of the recovered input images is substantially improved. On different underwater images from the UIEB dataset [24]we compare various underwater image processing methods and present the findings. These approaches consist of the following:These methods include UDCP [22], RBE [19], GBDRC [3], Water-net [24], ULAP [16], UWCNN [25].

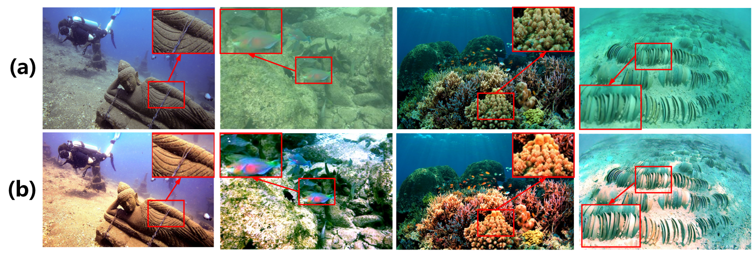

Fig. 7. Local details comparison test. (a) Input image, (b) Our results.

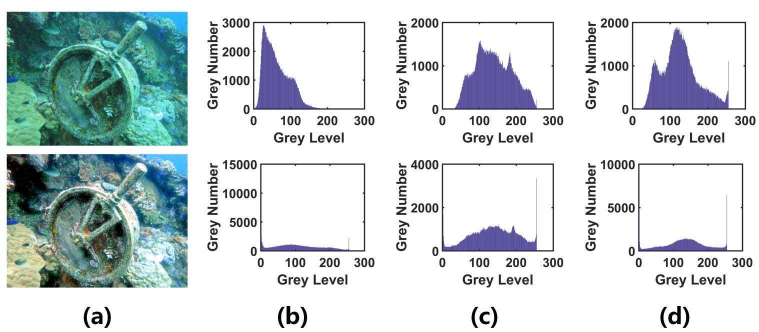

Fig. 8. (a) Original image and the restored image. Comparison of histograms of different channels restoration: (b) R channel, (c) G channel, (d) B channel.

4.1 Qualitative comparison

As displayed in Fig. 9(b), due to the overcompensation of red light, the restoration result of UDCP [22] is reddish. The restored images of RBE successfully reduces color cast and improves contrast, but it also generates a significant amount of black artifacts since it modifies the pixels without taking into account the causes of the deterioration. Low contrast can be seen in Fig. 9(e) and Fig. 9 (g) of the results produced by Water-net and UWCNN. Our method successfully raises the contrast of the image, as seen in Fig. 9(h). Fig. 9(d) presents the underwater image restoration results of the GBDRC [3] method. The restored images of GBDRC [3] introduce a more severe color shift. Due to the limited enhancement effect of the red channel, it usually leads to over-saturation of red in the restoration results. ULAP method fails to remove color distortion in green-hued underwater scenes. It is not as good as the proposed method in terms of contrast and color saturation.

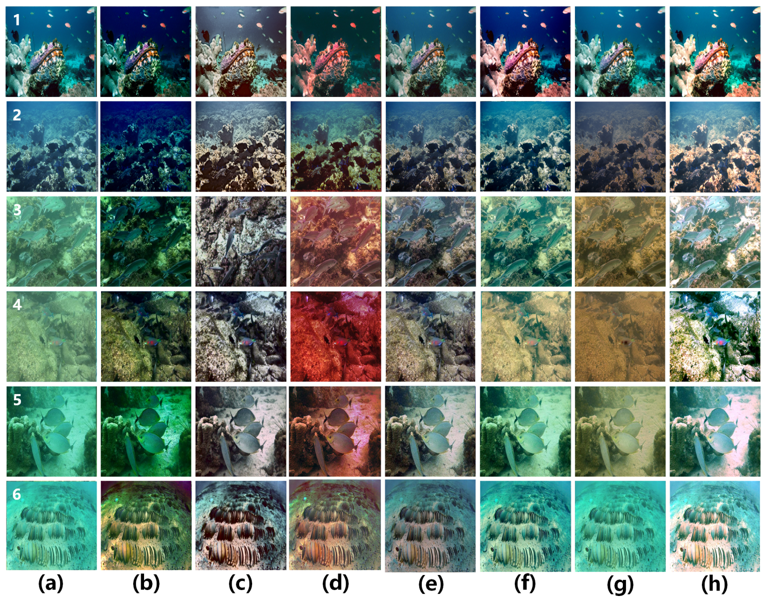

Fig. 9. Qualitative comparison of image enhancement between proposed and state-of-the-art methods. (a) Original image, (b) UDCP [22], (c) RBE [19], (d) GBDRC [3], (e) Water-net [24], (f) ULAP [16], (g) UWCNN [25], (h) Our method.

Additionally, in order to more fairly assess the effectiveness and dependability of the method, we compare the underwater images of more scenes in the UIEB dataset based on UDCP [22], RBE [19], GBDRC [3], Water-net [24], ULAP [16], UWCNN [25] and the proposed method in Fig.10. The methods vary in their ability to enhance the clarity and contrast of underwater photos, but the restoration results (Fig.10(b) and Fig.10(d)) of UDCP and GBDRC did not successfully eliminate the color deviation. Water-Net has a superior restoration impact and preserves more features, as demonstrated in Fig. 10(e), however, there is still some discrepancy with the restoration results of this paper. Compared to Water-Net, which creates underwater images with poor lighting, this algorithm's color and contrast are richer and more vivid. As shown in Fig. 10(c), RBE gives the recovery results of black artifacts. The clarity and color saturation of the results obtained by the ULAP method is not comparable to our method.

In conclusion, it can be seen from the comparison in various environments that the restoration results of the algorithm in this paper not only have the highest contrast and color saturation but also successfully preserve edge details and alter the distortions of the initial image to get better visual performance.

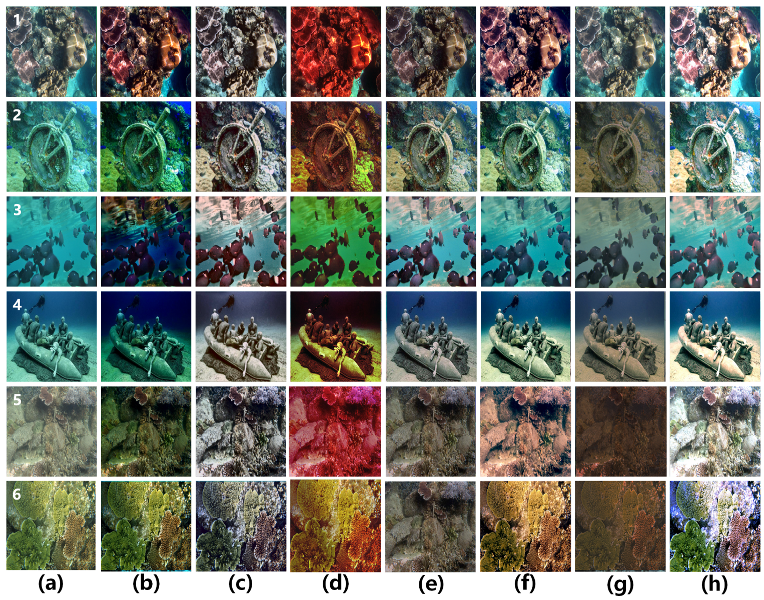

Fig. 10. Qualitative comparison of image enhancement between proposed and state-of-the-art methods. (a) Original image, (b) UDCP [22], (c) RBE [19], (d) GBDRC [3], (e) Water-net [24], (f) ULAP [16], (g) UWCNN [25], (h) Our method.

4.2 Quantitative Evaluation

In this paper, we use the following metrics to evaluate the quality of underwater images: underwater image quality assessment metrics UCIQE [31], AG, EI, and UIQM [32]. Table 1 shows the evaluation metrics results obtained after the complete UIEB dataset [24] is processed by our method. Four metrics of our method rank in the top three among all methods, especially UCIQE, AG, and EI rank first. The images from the UIEB [24] dataset demonstrate our supremacy.

The findings show that the UCIQE [31], UIQM [32], AG, and EI of the method are more robust than the other approaches, indicating that our method can effectively improve the color saturation and texture details of images. RBE does not consider the degradation of underwater images, resulting in artifacts and noise in the restoration results. The image effect can be slightly reduced by using the objective measurements of GBDRC, but the color distortion still cannot be precisely corrected. Water-net, a deep learning-based solution, performs

Table 1. COMPARISON OF THE AVERAGE METRICS OF UIEB IMAGES

	UDCP	RBE	GBDRC	Water-net	ULAP	UWCNN	Ours
UCIQE	0.5815	0.6023	0.5926	0.5839	0.6053	0.4765	**0.6215**
AG	5.1844	6.8699	4.6630	3.0843	6.0374	3.0843	**7.3144**
UIQM	**1.6459**	1.4073	1.4285	1.3647	1.4100	1.1047	1.4121
EI	51.066	70.765	45.963	57.864	59.414	30.308	**72.173**

badly. The method suggested in this paper has superior contrast. The restoration results of UWCNN show that the method will lead to more serious color casts in underwater images, and the results of UDCP are over-saturated with blue and green because only blue and green channels are considered in the restoration. Compared to previous methods, the restoration images produced by our solution often have greater visual quality and a better balance between the detail texture richness, color fidelity, and visual visibility of an image. The evaluation results on different metrics also provide convincing for the robustness and effectiveness of our method in recovering images with various scenes.

5 Conclusion

This research proposes an approach for underwater image restoration based on color floating and light attenuation. First, we provide a background light (BL) estimation model that takes into account hue, depth, entropy and chromatic aberration. Color casts in underwater images can be successfully removed by using accurate background lighting. Then, using the depth map to compute a new red channel transmission map (TM) estimationwe successfully increase image contrast while maintaining detailed information. In-depth analyses show the success of the background light estimating technique, the accuracy of the depth map method estimation, and the superiority of our method.

References

1. Li, C., Guo, J., Guo, C.: Emerging from water: Underwater image color correction based on weakly supervised color transfer. IEEE Signal Processing Letters **25**(3), 323–327 (2018)
2. Lin, Y., Zhou, J., Ren, W., Zhang, W.: Autonomous underwater robot for underwater image enhancement via multi-scale deformable convolution network with attention mechanism. Computers and Electronics in Agriculture **191**, 106497 (2021)
3. Li, C., Quo, J., Pang, Y., Chen, S., Jian, W.: Single underwater image restoration by blue-green channels dehazing and red channel correction. In: 2016 IEEE International Conference on Acoustics, Speech and Signal Processing (ICASSP) (2016)
4. Zhou, J., Yang, T., Ren, W., Zhang, D., Zhang, W.: Underwater image restoration via depth map and illumination estimation based on single image. Optics Express **29**(19) (2021)

5. Zhou, J.C., Zhang, D.H., Zhang, W.S.: Classical and state-of-the-art approaches for underwater image defogging: a comprehensive survey. Frontiers of Information Technology & Electronic Engineering **21**(12), 1745–1769 (2020)
6. Liu, R., Jiang, Z., Yang, S., Fan, X.: Twin adversarial contrastive learning for underwater image enhancement and beyond. IEEE Trans. Image Process. **31**, 4922–4936 (2022)
7. Zhou, J., Zhang, D., Ren, W., Zhang, W.: Auto color correction of underwater images utilizing depth information. IEEE Geosci. Remote. Sens. Lett. **19**, 1–5 (2022)
8. Zhou, J., Yang, T., Chu, W., Zhang, W.: Underwater image restoration via backscatter pixel prior and color compensation. Eng. Appl. Artif. Intell. **111**, 104785 (2022)
9. Anwar, S., Li, C.: Diving deeper into underwater enhancement: A survey. Signal Process. Image Commun. **89**, 115978 (2019)
10. Zhuang, P., Wu, J., Porikli, F., Li, C.: Underwater image enhancement with hyper-laplacian reflectance priors. IEEE Trans. Image Process. **31**, 5442–5455 (2022)
11. Jiang, Z., Li, Z., Yang, S., Fan, X., Liu, R.: Target oriented perceptual adversarial fusion network for underwater image enhancement. IEEE Transactions on Circuits and Systems for Video Technology (2022)
12. Peng, Y.T., Cosman, P.C.: Underwater image restoration based on image blurriness and light absorption. IEEE Trans Image Process **26**(4), 1579–1594 (2017)
13. He, K., Sun, J., Tang, X.: Single image haze removal using dark channel prior. IEEE Transactions on Pattern Analysis & Machine Intelligence **33**(12), 2341–2353 (2011)
14. Peng, Y., Cao, K., Cosman, P.C.: Generalization of the dark channel prior for single image restoration. IEEE Trans. Image Process. **27**(6), 2856–2868 (2018)
15. Nicholas, C.B., Anush, M., Eustice, R.M.: Initial results in underwater single image dehazing. In: Washington State Conference and Trade Center (WSCTC) (2010)
16. Song, W., Wang, Y., Huang, D., Tjondronegoro, D.: A rapid scene depth estimation model based on underwater light attenuation prior for underwater image restoration. In: Advances in Multimedia Information Processing (2018)
17. Zhuang, P., Li, C., Wu, J.: Bayesian retinex underwater image enhancement. Engineering Applications of Artificial Intelligence **101**(1), 104171 (2021)
18. Huang, D., Wang, Y., Song, W., Sequeira, J., Mavromatis, S.: Shallow-water image enhancement using relative global histogram stretching based on adaptive parameter acquisition. In: International Conference on Multimedia Modeling (2018)
19. Fu, X., Zhuang, P., Yue, H., Liao, Y., Zhang, X.P., Ding, X.: A retinex-based enhancing approach for single underwater image. In: 2014 IEEE International Conference on Image Processing (ICIP) (2015)
20. Lee, H.S., Sang, W.M., Eom, I.K.: Underwater image enhancement using successive color correction and superpixel dark channel prior. Symmetry **12**(8), 1220 (2020)
21. Zhou, J., Liu, Z., Zhang, W., Zhang, D., Zhang, W.: Underwater image restoration based on secondary guided transmission map. Multim. Tools Appl. **80**(5), 7771–7788 (2021)
22. Drews, J.P., Nascimento, E., Moraes, F., Botelho, S., Campos, M.: Transmission estimation in underwater single images. In: IEEE International Conference on Computer Vision Workshops (2013)
23. Galdran, A., Pardo, D., Picón, A., Alvarez-Gila, A.: Automatic red-channel underwater image restoration. Journal of Visual Communication & Image Representation **26**, 132–145 (2015)

24. Li, C., Guo, C., Ren, W., Cong, R., Hou, J., Kwong, S., Tao, D.: An underwater image enhancement benchmark dataset and beyond. IEEE Transactions on Image Processing **29**, 4376–4389 (2020)
25. Li, C., Anwar, S.: Underwater scene prior inspired deep underwater image and video enhancement. Pattern Recognition **98**(1), 107038 (2019)
26. Li, C., Anwar, S., Hou, J., Cong, R., Ren, W.: Underwater image enhancement via medium transmission-guided multi-color space embedding. IEEE Transactions on Image Processing **30**, 4985–5000 (2021)
27. Zhu, Q., Mai, J., Shao, L.: A fast single image haze removal algorithm using color attenuation prior. IEEE Transactions on Image Processing **24**(11), 3522–3533 (2015)
28. Chiang, J.Y., Chen, Y.C.: Underwater image enhancement by wavelength compensation and dehazing **21**(4), 1756–1769 (2012)
29. Zhao, X., Jin, T., Qu, S.: Deriving inherent optical properties from background color and underwater image enhancement. Ocean Engineering **94**, 163–172 (2015)
30. Song, W., Wang, Y., Huang, D., Liotta, A., Perra, C.: Enhancement of underwater images with statistical model of background light and optimization of transmission map. IEEE Transactions on Broadcasting **66**(1), 153–169 (2020)
31. Miao, Yang, Arcot, Sowmya: An underwater color image quality evaluation metric. IEEE Trans Image Process. **24**(12), 6062–6071 (2015)
32. Panetta, K., Gao, C., Agaian, S.: Human-visual-system-inspired underwater image quality measures. IEEE Journal of Oceanic Engineering **41**(3), 541–551 (2016)